Letter

Classical $\mathbb{Z}_2$ spin liquid on the generalized four-color Kitaev model

Han Yan (闫寒)[1,*] and Rico Pohle[2,3,4,†]

[1]Institute for Solid State Physics, The University of Tokyo, Kashiwa, Chiba 277-8581, Japan
[2]Institute for Materials Research, Tohoku University, Sendai, Miyagi 980-8577, Japan
[3]Graduate School of Science and Technology, Keio University, Hiyoshi, Yokohama 223-8522, Japan
[4]Department of Applied Physics, The University of Tokyo, Hongo, Tokyo 113-8656, Japan

(Received 21 September 2024; accepted 27 January 2025; published 4 March 2025)

While $U(1)$ spin liquids have been extensively studied in both quantum and classical regimes, exact classical $\mathbb{Z}_2$ spin liquids arising from models with nearest-neighbor, bilinear spin interactions are still rare. In this Letter, we explore the four-color Kitaev model as a minimal model for stabilizing classical $\mathbb{Z}_2$ spin liquids across a broad family of tricoordinated lattices. By formulating a $\mathbb{Z}_2$ lattice gauge theory, we identify this spin liquid as being described by an emergent Gauss's law with effective charge-2 condensation, and deconfined fractionalized bond-charge excitations. We complement our findings with Monte Carlo simulations, revealing a crossover from a high-temperature paramagnet to a low-temperature liquid phase characterized by residual entropy, classical $\mathbb{Z}_2$ flux order, and diffuse spin structure factors.

DOI: 10.1103/PhysRevResearch.7.L012052

Introduction. Lattice gauge theories, originally introduced by Wegner in 1971 [1], provided the first rigorous mathematical framework for describing emergent phenomena such as topological order. Over the years, lattice gauge theories have become essential for understanding a wide range of exotic phenomena in condensed matter physics, including the toric code [2], $\mathbb{Z}_2$ flux excitations in the Kitaev spin liquid [3,4], and resonating valence bond (RVB) liquids [5–7], bridging diverse topics, from the fundamentals of quantum computing [2,8] to superconductivity [9,10].

Spin liquids, strongly correlated systems that defy the conventional Landau paradigm of phase transitions, are typically studied in either their quantum or classical regime and are deeply tied to lattice gauge theoretical concepts [11]. In the classical regime, they exhibit an extensive ground-state degeneracy, often described by emergent electrostatics [12–15], while in the quantum regime, they may host phenomena such as topological order, topological entanglement entropy, and fractionalized excitations [16–18]. Although classical spin liquids lack long-range quantum entanglement, they can often serve as a foundation for constructing quantum spin liquids. A well-known example is spin ice, which realizes $U(1)$ Maxwell electrostatics [19–22] and transforms into quantum spin ice upon introducing quantum dynamics [23–25].

Building on the fundamental importance of classical spin liquids and the recent advances in demonstrating $\mathbb{Z}_2$ quantum spin liquids with Rydberg atoms [26–30], we propose a realistic classical spin model that explicitly realizes $\mathbb{Z}_2$ electrostatics. While many examples of classical $\mathbb{Z}_2$ spin liquids are built from dimer liquids that emerge from microscopic spin models [5,31–33], their direct realization from nearest-neighbor, bilinear spin interactions with an exact ground-state degeneracy remains exceedingly rare [34] and experimentally challenging to achieve [35]. Encouragingly, recent semiclassical simulations of the $S = 1$ Kitaev model, with finite bilinear and biquadratic spin interactions, have revealed a novel chiral spin liquid [36,37]. This state is characterized by a residual entropy, extremely short-ranged spin correlations, and nonzero scalar spin chirality marked by $\mathbb{Z}_2$ flux order—all properties that suggest it may represent a classical $\mathbb{Z}_2$ liquid. However, despite its discovery, a thorough analysis of the underlying gauge structure remains an open question.

In this Letter, we present the four-color Kitaev model, which realizes a broad family of classical $\mathbb{Z}_2$ spin liquids. By mapping spin degrees of freedom to local charges that act as sources of electric field fluxes, we show that this spin liquid is governed by an emergent Gauss's law with charge mod 2 as the ground-state condition. While different ground states within or across topological sectors are connected through loop updates, single-spin flips generate two fractional deconfined flux charges on bonds. We argue that the physics generally applies to tricoordinated lattices, which we explicitly validate on the honeycomb, square-octagon, and star lattices. We complement our results by finite-temperature Monte Carlo simulations, which reveal an almost lattice-independent crossover from a high-temperature paramagnet to a low-temperature liquid phase characterized by residual entropy, classical $\mathbb{Z}_2$ flux order, and diffuse spin structure factors. Our paper provides a detailed explanation of the underlying gauge structure of the chiral spin liquid found on the $S = 1$ Kitaev model with bilinear-biquadratic interactions,

*Contact author: hanyan@issp.u-tokyo.ac.jp
†Contact author: rico.pohle@tohoku.ac.jp

Published by the American Physical Society under the terms of the Creative Commons Attribution 4.0 International license. Further distribution of this work must maintain attribution to the author(s) and the published article's title, journal citation, and DOI.

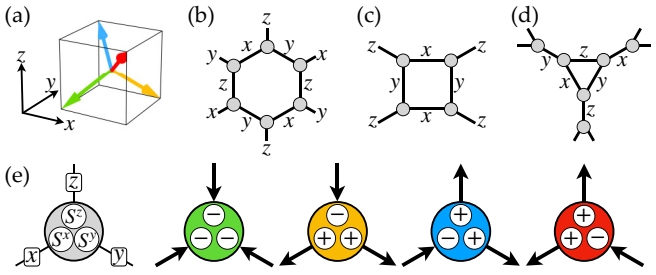


FIG. 1. Definition of spin directions in the four-color model with mapping to their effective lattice gauge theory. (a) Four considered discrete spin states with their corresponding colors. Kitaev bond labels are shown for the tricoordinated (b) honeycomb, (c) square-octagon, and (d) star lattices. (e) One-to-one mapping of individual spins to their charge degree of freedom. Every site contains three charges with flux lines pointing along the x, y, and z Kitaev bonds, according to the sign of their respective spin components S^x, S^y, and S^z.

as described in Refs. [36,37], and offers a framework for studying a broader class of classical $\mathbb{Z}_2$ spin liquids.

The four-color Kitaev model. We consider classical, discretized spins oriented towards four of the eight corners of a unit cube, defined as follows:

$$\begin{aligned} \text{green}: &\quad \vec{S}_\text{g} = \tfrac{1}{\sqrt{3}}\{-1,-1,-1\}\,, \\ \text{yellow}: &\quad \vec{S}_\text{y} = \tfrac{1}{\sqrt{3}}\{+1,+1,-1\}\,, \\ \text{blue}: &\quad \vec{S}_\text{b} = \tfrac{1}{\sqrt{3}}\{-1,+1,+1\}\,, \\ \text{red}: &\quad \vec{S}_\text{r} = \tfrac{1}{\sqrt{3}}\{+1,-1,+1\}\,. \end{aligned} \tag{1}$$

The color assignments ("green", "yellow", "blue", and "red") and spin directions follow the convention used in Refs. [36,37] and are illustrated in Fig. 1(a). The four-color state arises in various contexts: It does not only describe the low-temperature physics of the $S = 1$ model studied in Refs. [36,37], but also serves as the simplest discretization of $O(3)$ vector spins. Various microscopic models with similar four-dimensional local degree of freedom have been studied [38–42], making it particularly compelling to investigate its behavior on the Kitaev model.

We consider models with Kitaev-type bond-anisotropic spin interactions defined on tricoordinated lattices. In such lattices every site is connected to its neighbors by three distinct types of bonds, typically labeled as x, y, and z, ensuring that each site has exactly one bond of each kind.

The Hamiltonian defined on these lattices is

$$\mathscr{H}_\text{4c} = \sum_{\alpha=x,y,z} \sum_{\langle ij\rangle_\alpha} S_i^\alpha S_j^\alpha\,, \tag{2}$$

with S_i^α being the $\alpha = x, y, z$ component of a discrete vector spin at site i in one of the four states shown in Eq. (1). Throughout this paper, we refer to this model as the "four-color model," where interactions occur solely for the α spin components on the $\langle ij\rangle_\alpha$ Kitaev bonds. We exemplify our study on three tricoordinated lattices in two dimensions, namely the honeycomb, square-octagon, and star lattices, with their corresponding Kitaev-bond labels shown in Figs. 1(b)–1(d), respectively.

The ground state of the four-color model in Eq. (2) is obtained by minimizing the energy on each Kitaev bond without frustration between different bonds. Local energies are minimized for multiple configurations of color pairs.

On the x bonds:

$$(\vec{S}_\text{g}, \vec{S}_\text{y}), (\vec{S}_\text{g}, \vec{S}_\text{r}), (\vec{S}_\text{b}, \vec{S}_\text{y}), (\vec{S}_\text{b}, \vec{S}_\text{r}). \tag{3}$$

On the y bonds:

$$(\vec{S}_\text{g}, \vec{S}_\text{y}), (\vec{S}_\text{g}, \vec{S}_\text{b}), (\vec{S}_\text{r}, \vec{S}_\text{y}), (\vec{S}_\text{r}, \vec{S}_\text{b}). \tag{4}$$

On the z bonds:

$$(\vec{S}_\text{g}, \vec{S}_\text{b}), (\vec{S}_\text{g}, \vec{S}_\text{r}), (\vec{S}_\text{y}, \vec{S}_\text{b}), (\vec{S}_\text{y}, \vec{S}_\text{r}). \tag{5}$$

These configurations set the ground-state bond constraints, which are not strong enough to enforce long-range order but instead lead to a classical spin-liquid state with extensively many degenerate ground states, as discussed in detail for the eight-color model in Ref. [37] on the honeycomb lattice.

Emergent $\mathbb{Z}_2$ gauge structure. While Eqs. (3)–(5) completely determine all the ground states of $\mathscr{H}_\text{4c}$ in Eq. (2), the nature of the corresponding spin liquids and their field-theoretical interpretation are still unknown. In the following, we investigate these aspects by formulating a $\mathbb{Z}_2$ lattice gauge theory for this spin liquid.

We construct an equivalent model that treats each spin as a source of three electric field fluxes. As illustrated in Fig. 1(e), we assign fluxes to individual Kitaev bonds according to the components of each spin at the vertex. For a spin vector $\vec{S} = \{S^x, S^y, S^z\}$, the assigned flux along the α bond is $(\sqrt{3}/2)S^\alpha$, whose normalization coefficient $\sqrt{3}/2$ ensures a net flux change in units of ± 1. This corresponds to a charge contribution of $\pm 1/2$ to the vertex from each spin component, resulting in the total charge of $-3/2$ for $\vec{S}_\text{g}$ and $+1/2$ for $\vec{S}_\text{y}$, $\vec{S}_\text{b}$ and $\vec{S}_\text{r}$. In visual representations, we use "arrows" to illustrate "electric field fluxes".

In the ground state, two adjacent sites connected by a bond must also share aligned electric field fluxes to minimize the bond energy $S_i^\alpha S_j^\alpha$. This ensures there is no net charge on the bond center, consistent with the ground-state constraints outlined in Eqs. (3)–(5). Each ground state is then mapped to a unique configuration of electric field fluxes on the lattice, whose vertex charges can be either $-3/2$ or $1/2$. On the other hand, for every flux configuration with zero charge on bond centers, there exists a corresponding unique ground-state spin configuration, as long as each vertex conforms to the configurations listed in Fig. 1(e). While the bond centers remain charge-neutral, each vertex can take a charge of either $-3/2$ or $+1/2$. This condition implies the $\mathbb{Z}_2$ Gauss's law at each vertex [31],

$$\nabla \cdot \boldsymbol{E} = -3/2 \text{ or } 1/2\,. \tag{6}$$

The crucial point is that the allowed charges satisfy the condition $-3/2 = 1/2 \mod 2$. This indicates that the system can change its charge by even numbers and still remains in the ground state, but not by odd numbers. Such a concept resembles classical "charge condensation", where condensation of

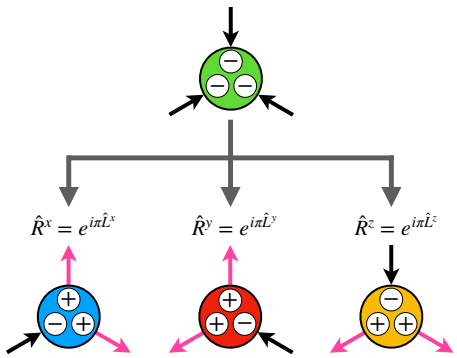


FIG. 2. Single-spin update demonstrated for a green spin $\vec{S}_g$ as defined in Eq. (1). Rotation operators $\hat{R}^\alpha$ [see Eq. (7)] with $\alpha = x, y, z$, preserve the flux on the α Kitaev bond while inverting the flux on the other two bonds. Such an update violates the bond-flux constraint [see Fig. 1(e) and Eq. (6)] and creates excitations when acted on a ground state.

charge-2 particles in $U(1)$ gauge theories yields a $\mathbb{Z}_2$ gauge theory, which is characterized by gapped topological order [2,31,34]. Consequently, the $U(1)$ Gauss's law, $\nabla \cdot \boldsymbol{E} = 0$, transforms to $\nabla \cdot \boldsymbol{E} = 0 \mod 2$. Equation (6) captures the essence of this law, albeit a nonzero background charge of $1/2$, with allowed charges being only limited to $-3/2$ and $1/2$, rather than all the numbers equivalent to $1/2 \mod 2$.

$\mathbb{Z}_2$ topological sectors. To understand the structure of the topological sectors in the spin-liquid ground state of $\mathscr{H}_{4c}$ [see Eq. (2)] we investigate how different ground states are connected via local and nonlocal loop updates of spins. We start by discussing single-spin flip updates, as exemplified for $\vec{S}_g$ in Fig. 2. In the spin representation, updating a single spin is equivalent to applying the rotation operator

$$\hat{R}^\alpha = e^{i\pi\hat{L}^\alpha}, \tag{7}$$

where $\hat{L}^\alpha$ is the generator of $SO(3)$ rotations. The operator $\hat{R}^\alpha$ rotates the spin by an angle π around the α axis, keeping the spin within the set of four color states.

In the electric field flux picture, $\hat{R}^\alpha$ leaves the flux on the α bond unchanged while reversing the fluxes on the other two bonds. Note that spins of different color always differ by two of the three electric field fluxes. Since such a local operation changes the flux on two bonds and creates charges on their bond centers, the new state is always an excited state. Therefore, single-spin updates do not connect different states in the ground-state manifold. To connect different spin configurations within the ground-state manifold, one requires multiple single-spin flips in the form of closed loops, as shown in explicit examples in Fig. 3. On the honeycomb lattice, the shortest loop is a hexagon. Performing such a loop update involves applying $\hat{R}^\alpha$ [see Eq. (7)] to each of the six sites within the hexagon, where α is the index of the Kitaev bond pointing outside the hexagon [see Fig. 3(a), left]. The corresponding operator

$$\hat{W}_p \equiv e^{i\pi\hat{L}^z_0} e^{i\pi\hat{L}^y_1} e^{i\pi\hat{L}^x_2} e^{i\pi\hat{L}^z_3} e^{i\pi\hat{L}^y_4} e^{i\pi\hat{L}^x_5} \tag{8}$$

acts locally in the bulk and connects different spin-liquid ground states within the same topological sector. We note that

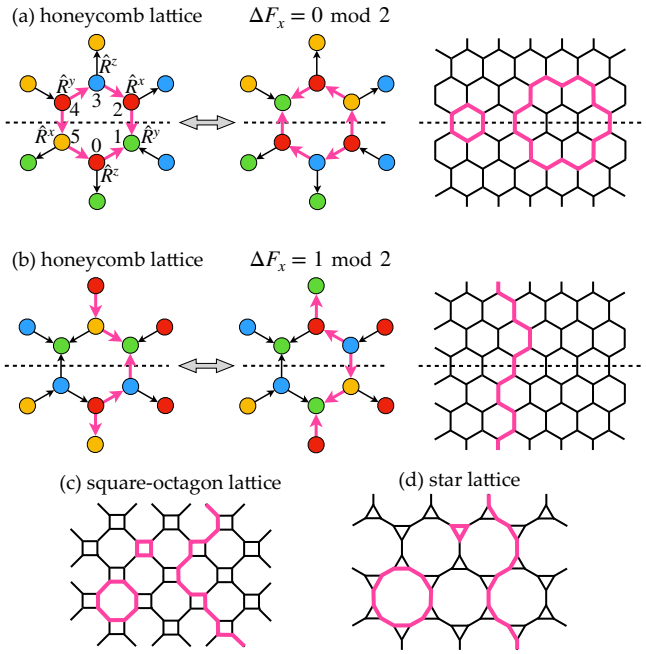


FIG. 3. Local and noncontractible loop updates connect states within the spin-liquid ground-state manifold of $\mathscr{H}_{4c}$ [see Eq. (2)]. These updates involve the successive application of rotation operators $\hat{R}^\alpha$ [see Eq. (7) and Fig. 2] on spins along loops, highlighted in pink. (a) For local loop updates on the honeycomb lattice, the change in flux along any closed loop within the bulk (depicted by a dashed-black line) takes values of $\Delta F_x = 0 \mod 2$. (b) For noncontractible loop updates, which wrap around the torus of the honeycomb lattice, $\Delta F_x = 1 \mod 2$, dividing the ground states into different topological sectors. Loops are defined in a similar way on other tricoordinated lattices, such as (c) the square-octagon lattice and (d) the star lattice.

$\hat{W}_p$ in Eq. (8) is exactly the "flux operator" in the original quantum Kitaev honeycomb model [3,4], if we turn the generators $\hat{L}^\alpha$ into quantum spin operators $\hat{S}^\alpha$. In general, Eq. (8) can be extended to any tricoordinate lattice with

$$\hat{W}_p \equiv \prod_{\{j,\alpha\}} e^{i\pi\hat{L}^\alpha_j}, \tag{9}$$

where the index j runs over loops of any size, such as 4 and 8 in the square-octagon lattice [see Fig. 3(c)], or 3 and 12 on the star lattice [see Fig. 3(d)].

To understand the topological sectors of the ground state, we analyze its degeneracy structure and explore how flipping of loops can connect different spin configurations. Given any ground-state configuration, flipping fluxes on a hexagon or other local loop always yields another ground state. This property arises from allowing the vertex charge to change only by units of ± 2 [see Eq. (6)]. Importantly, in these models, local loops are always flippable, and the fluxes do not need to connect head-to-tail as is required in $U(1)$ spin liquids to maintain a charge of 0 on every vertex [23,31,43].

We examine the total flux F_x along all bonds intersected by a straight line (analogous to a Wilson loop or topological number/logical qubit [2,44]) along the x direction on the honeycomb lattice [dashed line in Figs. 3(a) and 3(b)]. In Fig. 3(a), one observes that the change of flux (highlighted in

pink) before and after the cluster update of a single hexagon is either $\Delta F_x = \pm 2$ or $\Delta F_x = 0$ (not shown), since the straight line always intersects an even number of bonds. Accordingly, the total flux can only change by an even number $\Delta F_x = 0 \mod 2$ for any loop confined within the bulk of the system. All ground states connected by such local loop updates belong to the same topological sector labeled by the net flux $F_x \mod 2$ [2,31].

To alter the total flux $F_x \mod 2$, the loop must wrap around the torus of the lattice. Such a noncontractible loop intersects the straight line an odd number of times, as shown in Fig. 3(b), and changes the net flux by $\Delta F_x = 1 \mod 2$. Consequently, the system enters a different topological sector, which cannot be reached through local loop updates confined within the bulk. The same reasoning applies to other tricoordinated lattices, as visualized in Figs. 3(c) and 3(d). The noncontractible loop-flipping operator is analogous to the topological operator/logical gate [2,44].

On a torus, the total fluxes $F_{x,y}$ over the cuts in the x and y directions, being either odd or even, divide the ground states into four topological sectors. States in the same sector are connected via local loop updates, while those in different sectors are not. This is exactly the classical limit of gapped $\mathbb{Z}_2$ topological order [2]. In this context, local loop updates act as the analog of "magnetic field operators", leaving the system in the ground-state manifold by altering the electric field configuration without creating charges on the bond centers. On the other hand, noncontractible loop updates take the system ground state to a different topological sector [45].

$\mathbb{Z}_2$ charges. The lowest-energy excitations from the ground state are states with one charge on a bond. Flipping a single spin inverts the fluxes on two bonds (see Fig. 2), which creates two nonzero charges at the cost of $\Delta E = \frac{4}{3}$. Once created, these charges can move independently throughout the system via successive single-spin flips without any additional energy cost. Thus, such excitations form a classical analog of deconfined fractionalized excitations.

These fractional excitations behave like $\mathbb{Z}_2$ charges rather than $U(1)$ charges, meaning that only the charge $\mod 2$ is conserved, instead of the net charge itself. One can create two bond-center charges of either $(+1,+1)$, $(+1,-1)$ or $(-1,-1)$ by flipping a spin. As a charge moves around the lattice through successive single-spin flips, its $\pm$ sign can change. Consequently, for bond-center charges, only their even/oddness (i.e., charge $\mod 2$) is conserved, rather than the total charge. This characteristic is consistent with the defining feature of a $\mathbb{Z}_2$ spin liquid.

Finite-temperature properties. We complement our analytical understanding of the spin-liquid ground state in $\mathscr{H}_{4c}$ [see Eq. (2)] with finite-temperature Monte Carlo (MC) simulations. As discussed previously, single-spin flip updates alone are insufficient to thermalise the system at low temperatures. Therefore, we use a hybrid Monte Carlo scheme that combines single-spin flip updates with local loop updates. In this scheme, a single MC step consists of N_s (total site number) local Metropolis spin-flip attempts at randomly chosen sites of the lattice, followed by N_l (total number of elementary loops) cluster update attempts by applying Eq. (9) on randomly chosen elementary loops on the lattice. To further mitigate correlation times, we employ parallelization in temperature

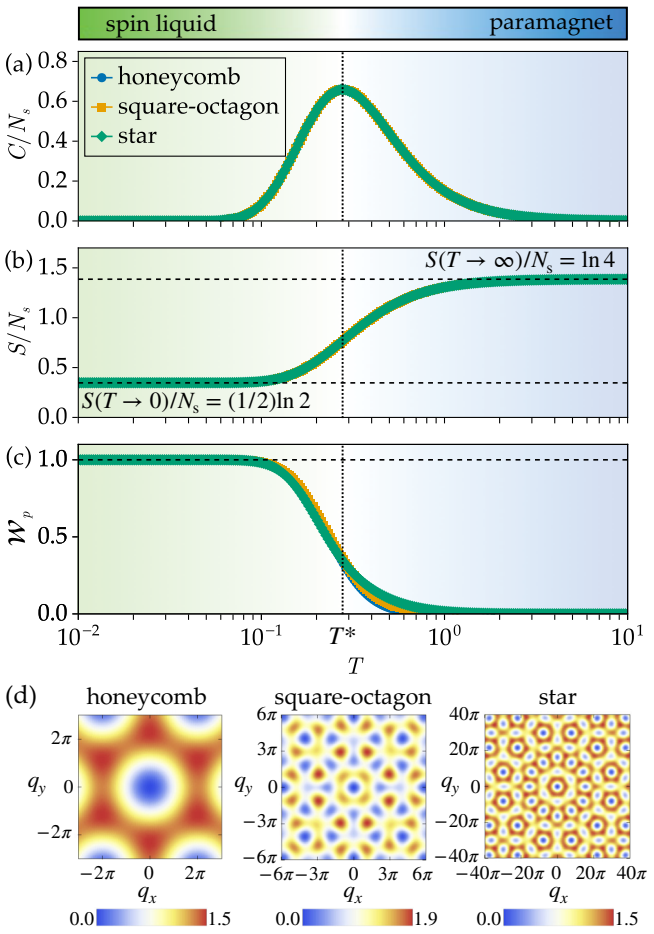


FIG. 4. Finite-temperature Monte Carlo simulations of $\mathscr{H}_{4c}$ [see Eq. (2)] on the honeycomb, square-octagon and star lattice, reveal a crossover from a high-temperature paramagnet to a low-temperature spin liquid. The panels depict normalized values for (a) the specific heat, C/N_s, (b) the thermodynamic entropy, S/N_s, and (c) the classical analog of the $\mathbb{Z}_2$-flux operator, $\mathcal{W}_p$ [see Eq. (10)]. Panel (d) shows the spin structure factor, $S(\mathbf{q})$, for all three lattice models in the spin-liquid phase at $T = 0.01$. Thermodynamic observables (spin structure factors) were obtained for finite-size clusters with periodic boundary conditions and linear dimensions of $L = 96$ ($L = 48$) for the honeycomb, $L = 60$ ($L = 24$) for the square-octagon, and $L = 60$ ($L = 12$) for the star lattice models.

using the replica-exchange algorithm [46] every 100 MC steps. Thermodynamic quantities are averaged over 5×10^5 statistically independent samples, after 1×10^6 steps of simulated annealing and thermalization each.

In Fig. 4, we show finite-temperature MC simulation results of $\mathscr{H}_{4c}$ [Eq. (2)] for honeycomb, square-octagon, and star lattice models. The specific heat exhibits a lattice independent crossover from a high-temperature paramagnet to the low-temperature spin liquid with a broad peak spanning over one order of magnitude in temperature, and a peak maximum at $T^* = 0.272(8)$. We note that the four-color model itself explicitly breaks the time-reversal symmetry by considering only four allowed spin states, as illustrated in Fig. 1(a). Consequently, we do not observe a finite-temperature phase transition, in contrast to the observations in Ref. [37], which

investigates the time-reversal symmetric case involving eight states.

Upon cooling, the system releases its thermodynamic entropy, $S(T \to \infty)/N_s = \ln 4$, to a residual value of $S(T \to 0)/N_s = \frac{1}{2}\ln 2$. This residual entropy reflects the remaining degeneracy in the ground state, counting always two possible configurations for every elementary loop in the lattice. A similar behavior is observed in the classical analog of the $\mathbb{Z}_2$-flux operator $\mathcal{W}_p$,

$$\mathcal{W}_p = \prod_{j\in p} \sqrt{3} S_j^{\alpha}\,, \tag{10}$$

which is not an operator per se but rather a quantity that evaluates whether the Gauss's law [Eq. (6)] is globally satisfied or not. Upon cooling, $\mathcal{W}_p$ gradually increases within the crossover window, eventually reaching a value of $+1$ at low temperatures.

Characteristic magnetic scattering signatures in the spin-liquid phase of all three lattice models are shown in the energy-integrated structure factors $S(\mathbf{q})$ in Fig. 4(d). The signal for all lattice models is very diffuse, directly indicating the absence of any conventional magnetic order. The absence of singularities, such as "pinch-points", characteristic of Coulombic $U(1)$ liquids, stems from the underlying $\mathbb{Z}_2$ Gauss law in Eq. (6). Consequently, this spin liquid belongs to the category of fragile topological spin liquids [13,14], characterized by a gapped spectrum of the interaction matrix and exponentially decaying spin-spin correlations. Notably, these spin-spin correlations are extremely short ranged, aligning with analytical predictions for the $S = 1$ Kitaev spin liquid in Ref. [4]. While the honeycomb lattice exhibits a periodic structure with dominant weight concentrated near the Brillouin zone edges, the square-octagon and star lattices display an aperiodic pattern. This aperiodicity originates from the fractional distances of real-space lattice sites and has also been observed in other spin liquids, e.g., on the ruby lattice [34] or the square-kagome lattice [47].

Conclusions and discussion. We have studied the generalized four-color Kitaev model and demonstrated that it stabilizes a classical $\mathbb{Z}_2$ spin liquid across a broad family of tricoordinated lattices. By developing an effective $\mathbb{Z}_2$ lattice gauge theory for this family of models, we identified an emergent Gauss's law, constrained to charge mod 2, as the ground-state condition, leading to the formation of topological sectors and deconfined bond-charge excitations.

Our paper offers a significant contribution to the search for exotic spin liquids, particularly those exhibiting Kitaev-type anisotropies. Moreover, it represents a rare example of a $\mathbb{Z}_2$ classical liquid directly realized in a model with bilinear spin interactions, rather than as an emergent form of a dimer liquid or from models with multispin interactions.

The most promising place to look for a realization of this $\mathbb{Z}_2$ spin liquid may lie in $S = 1$ Kitaev models on the honeycomb lattice with additional bilinear-biquadratic spin interactions, as studied in Refs. [36,37]. In those studies, semiclassical simulations demonstrated that the right balance of dominant Kitaev and finite bilinear-biquadratic interactions stabilizes a finite-temperature chiral spin liquid. The physics of this liquid can be effectively captured by the four-color model given in Eq. (2). Potential experimental realizations might be found in honeycomb materials composed of Ni^{2+} ions [48], where positive biquadratic interactions may arise from orbital degeneracy [49–51].

While the conclusions presented in this paper generally apply to tricoordinated lattices, we have made our discussions explicit on only three lattice models in two dimensions: the honeycomb, square-octagon, and star lattice. We believe an extension to tricoordinate lattices in three dimensions is straightforward and offers another promising route to discover exotic spin liquids [52–55].

An important direction for future investigations is to explore the connection between our results and quantum models at zero temperature. The results in this paper, along with those in Refs. [36,37], primarily address classical physics, where quantum entanglement between spins is absent. While local perturbations in such classical models lift the degeneracy and lead the system into a long-range ordered phase, incorporating quantum dynamics—for example, through local loop operators such as the $\mathbb{Z}_2$-flux operator $\mathcal{W}_p$ in Eq. (9)—could potentially drive the system into topological order [33,56], which would be robust against perturbations. Furthermore, the connection between our results and quantum $S = 1$ Kitaev models [4,57–66], chiral spin liquids on tricoordinated lattices [61,67–72], quantum loop models [73], and $\mathbb{Z}_4$ Kitaev spin liquids [74], remains an open and fascinating question for future studies. In particular, we hope our results will provide valuable insights into the concrete construction of ground-state wave functions for high-spin quantum Kitaev models and their variants.

Acknowledgments. The authors are indebted to Yukitoshi Motome and Nic Shannon for helpful conversations and a critical reading of the manuscript. R.P. acknowledges support from the Quantum Liquid Crystals JSPS KAKENHI Grant No. JP19H05825, and MEXT as "Program for Promoting Researches on the Supercomputer Fugaku" (Grant No. JPMXP1020230411). H.Y. is supported by the 2024 Toyota Riken Scholar Program from the Toyota Physical and Chemical Research Institute, and the Grant-in-Aid for Research Activity Start-up from Japan Society for the Promotion of Science (Grant No. 24K22856). Numerical calculations were carried out using HPC facilities provided by the Supercomputer Center of the Institute for Solid State Physics, the University of Tokyo.

[1] F. J. Wegner, Duality in generalized Ising models and phase transitions without local order parameters, J. Math. Phys. **12**, 2259 (1971).

[2] A. Kitaev, Fault-tolerant quantum computation by anyons, Ann. Phys. (NY) **303**, 2 (2003).

[3] A. Kitaev, Anyons in an exactly solved model and beyond, Ann. Phys. (NY) **321**, 2 (2006).

[4] G. Baskaran, D. Sen, and R. Shankar, Spin-*S* Kitaev model: Classical ground states, order from disorder, and exact correlation functions, Phys. Rev. B **78**, 115116 (2008).

[5] R. Moessner and S. L. Sondhi, Resonating valence bond phase in the triangular lattice quantum dimer model, Phys. Rev. Lett. **86**, 1881 (2001).

[6] A. Ralko, M. Ferrero, F. Becca, D. Ivanov, and F. Mila, Zero-temperature properties of the quantum dimer model on the triangular lattice, Phys. Rev. B **71**, 224109 (2005).

[7] G. Misguich, D. Serban, and V. Pasquier, Quantum dimer model on the kagome lattice: Solvable dimer-liquid and Ising gauge theory, Phys. Rev. Lett. **89**, 137202 (2002).

[8] C. Nayak, S. H. Simon, A. Stern, M. Freedman, and S. Das Sarma, Non-Abelian anyons and topological quantum computation, Rev. Mod. Phys. **80**, 1083 (2008).

[9] T. Senthil and M. P. A. Fisher, Z_2 gauge theory of electron fractionalization in strongly correlated systems, Phys. Rev. B **62**, 7850 (2000).

[10] P. A. Lee, N. Nagaosa, and X.-G. Wen, Doping a Mott insulator: Physics of high-temperature superconductivity, Rev. Mod. Phys. **78**, 17 (2006).

[11] X.-G. Wen, *Quantum Field Theory of Many-Body Systems: From the Origin of Sound to an Origin of Light and Electrons* (Oxford University Press, Oxford, 2007).

[12] N. Davier, F. A. Gómez Albarracín, H. D. Rosales, and P. Pujol, Combined approach to analyze and classify families of classical spin liquids, Phys. Rev. B **108**, 054408 (2023).

[13] H. Yan, O. Benton, R. Moessner, and A. H. Nevidomskyy, Classification of classical spin liquids: Typology and resulting landscape, Phys. Rev. B **110**, L020402 (2024).

[14] H. Yan, O. Benton, A. H. Nevidomskyy, and R. Moessner, Classification of classical spin liquids: Detailed formalism and suite of examples, Phys. Rev. B **109**, 174421 (2024).

[15] Y. Fang, J. Cano, A. H. Nevidomskyy, and H. Yan, Classification of classical spin liquids: Topological quantum chemistry and crystalline symmetry, Phys. Rev. B **110**, 054421 (2024).

[16] L. Balents, Spin liquids in frustrated magnets, Nature (London) **464**, 199 (2010).

[17] L. Savary and L. Balents, Quantum spin liquids: A review, Rep. Prog. Phys. **80**, 016502 (2017).

[18] Y. Zhou, K. Kanoda, and T.-K. Ng, Quantum spin liquid states, Rev. Mod. Phys. **89**, 025003 (2017).

[19] M. J. Harris, S. T. Bramwell, D. F. McMorrow, T. Zeiske, and K. W. Godfrey, Geometrical frustration in the ferromagnetic pyrochlore $Ho_2Ti_2O_7$, Phys. Rev. Lett. **79**, 2554 (1997).

[20] R. Moessner and J. T. Chalker, Properties of a classical spin liquid: the Heisenberg pyrochlore antiferromagnet, Phys. Rev. Lett. **80**, 2929 (1998).

[21] R. Moessner and J. T. Chalker, Low-temperature properties of classical geometrically frustrated antiferromagnets, Phys. Rev. B **58**, 12049 (1998).

[22] M. Udagawa and L. Jaubert, *Spin Ice* (Springer International Publishing, Cham, 2021).

[23] M. Hermele, M. P. A. Fisher, and L. Balents, Pyrochlore photons: The $U(1)$ spin liquid in a $S = \frac{1}{2}$ three-dimensional frustrated magnet, Phys. Rev. B **69**, 064404 (2004).

[24] N. Shannon, O. Sikora, F. Pollmann, K. Penc, and P. Fulde, Quantum ice: A quantum Monte Carlo study, Phys. Rev. Lett. **108**, 067204 (2012).

[25] O. Benton, O. Sikora, and N. Shannon, Seeing the light: Experimental signatures of emergent electromagnetism in a quantum spin ice, Phys. Rev. B **86**, 075154 (2012).

[26] A. Keesling, A. Omran, H. Levine, H. Bernien, H. Pichler, S. Choi, R. Samajdar, S. Schwartz, P. Silvi, S. Sachdev *et al.*, Quantum Kibble-Zurek mechanism and critical dynamics on a programmable Rydberg simulator, Nature (London) **568**, 207 (2019).

[27] R. Samajdar, W. W. Ho, H. Pichler, M. D. Lukin, and S. Sachdev, Quantum phases of Rydberg atoms on a kagome lattice, Proc. Natl. Acad. Sci. USA **118**, e2015785118 (2021).

[28] R. Verresen, M. D. Lukin, and A. Vishwanath, Prediction of toric code topological order from Rydberg blockade, Phys. Rev. X **11**, 031005 (2021).

[29] G. Semeghini, H. Levine, A. Keesling, S. Ebadi, T. T. Wang, D. Bluvstein, R. Verresen, H. Pichler, M. Kalinowski, R. Samajdar *et al.*, Probing topological spin liquids on a programmable quantum simulator, Science **374**, 1242 (2021).

[30] S. Ebadi, T. T. Wang, H. Levine, A. Keesling, G. Semeghini, A. Omran, D. Bluvstein, R. Samajdar, H. Pichler, W. W. Ho *et al.*, Quantum phases of matter on a 256-atom programmable quantum simulator, Nature (London) **595**, 227 (2021).

[31] S. Sachdev and M. Vojta, Translational symmetry breaking in two-dimensional antiferromagnets and superconductors, J. Phys. Soc. Jpn. **99**, 1 (1999).

[32] R. Moessner and K. S. Raman, Quantum dimer models, in *Introduction to Frustrated Magnetism: Materials, Experiments, Theory*, edited by C. Lacroix, P. Mendels, and F. Mila (Springer, Berlin, 2011), pp. 437–479.

[33] R. Verresen and A. Vishwanath, Unifying Kitaev magnets, kagomé dimer models, and Ruby Rydberg spin liquids, Phys. Rev. X **12**, 041029 (2022).

[34] J. Rehn, A. Sen, and R. Moessner, Fractionalized $\mathbb{Z}_2$ classical Heisenberg spin liquids, Phys. Rev. Lett. **118**, 047201 (2017).

[35] J. Rehn, A. Sen, K. Damle, and R. Moessner, Classical spin liquid on the maximally frustrated honeycomb lattice, Phys. Rev. Lett. **117**, 167201 (2016).

[36] R. Pohle, N. Shannon, and Y. Motome, Spin nematics meet spin liquids: Exotic quantum phases in the spin-1 bilinear-biquadratic model with Kitaev interactions, Phys. Rev. B **107**, L140403 (2023).

[37] R. Pohle, N. Shannon, and Y. Motome, Eight-color chiral spin liquid in the $S = 1$ bilinear-biquadratic model with Kitaev interactions, Phys. Rev. Res. **6**, 033077 (2024).

[38] J. Ashkin and E. Teller, Statistics of two-dimensional lattices with four components, Phys. Rev. **64**, 178 (1943).

[39] J. Kondev and C. L. Henley, Four-coloring model on the square lattice: A critical ground state, Phys. Rev. B **52**, 6628 (1995).

[40] V. Khemani, R. Moessner, S. A. Parameswaran, and S. L. Sondhi, Bionic Coulomb phase on the pyrochlore lattice, Phys. Rev. B **86**, 054411 (2012).

[41] G.-W. Chern and C. Wu, Four-coloring model and frustrated superfluidity in the diamond lattice, Phys. Rev. Lett. **112**, 020601 (2014).

[42] D. Lozano-Gómez, Y. Iqbal, and M. Vojta, A classical chiral spin liquid from chiral interactions on the pyrochlore lattice, Nat. Commun. **15**, 10162 (2024).

[43] D. A. Huse, W. Krauth, R. Moessner, and S. L. Sondhi, Coulomb and liquid dimer models in three dimensions, Phys. Rev. Lett. **91**, 167004 (2003).

[44] M. A. Nielsen and I. L. Chuang, *Quantum Computation and Quantum Information* (Cambridge University Press, Cambridge, 2000).

[45] E. Dennis, A. Kitaev, A. Landahl, and J. Preskill, Topological quantum memory, J. Math. Phys. **43**, 4452 (2002).
[46] R. H. Swendsen and J.-S. Wang, Replica Monte Carlo simulation of spin-glasses, Phys. Rev. Lett. **57**, 2607 (1986).
[47] R. Pohle, O. Benton, and L. D. C. Jaubert, Reentrance of disorder in the anisotropic shuriken Ising model, Phys. Rev. B **94**, 014429 (2016).
[48] P. P. Stavropoulos, D. Pereira, and H.-Y. Kee, Microscopic mechanism for a higher-spin Kitaev model, Phys. Rev. Lett. **123**, 037203 (2019).
[49] A. Yoshimori and S. Inagaki, Fourth order interaction effects on the antiferromagnetic structures. II. A phenomenological model for NiS_2, J. Phys. Soc. Jpn. **50**, 769 (1981).
[50] M. Hoffmann and S. Blügel, Systematic derivation of realistic spin models for beyond-Heisenberg solids, Phys. Rev. B **101**, 024418 (2020).
[51] R. Soni, N. Kaushal, C. Sen, F. A. Reboredo, A. Moreo, and E. Dagotto, Estimation of biquadratic and bicubic Heisenberg effective couplings from multiorbital Hubbard models, New J. Phys. **24**, 073014 (2022).
[52] S. Mandal and N. Surendran, Exactly solvable Kitaev model in three dimensions, Phys. Rev. B **79**, 024426 (2009).
[53] K. O'Brien, M. Hermanns, and S. Trebst, Classification of gapless $\mathbb{Z}_2$ spin liquids in three-dimensional Kitaev models, Phys. Rev. B **93**, 085101 (2016).
[54] T. Eschmann, P. A. Mishchenko, K. O'Brien, T. A. Bojesen, Y. Kato, M. Hermanns, Y. Motome, and S. Trebst, Thermodynamic classification of three-dimensional Kitaev spin liquids, Phys. Rev. B **102**, 075125 (2020).
[55] P. A. Mishchenko, Y. Kato, K. O'Brien, T. A. Bojesen, T. Eschmann, M. Hermanns, S. Trebst, and Y. Motome, Chiral spin liquids with crystalline $\mathbb{Z}_2$ gauge order in a three-dimensional Kitaev model, Phys. Rev. B **101**, 045118 (2020).
[56] P. S. Tarabunga, F. M. Surace, R. Andreoni, A. Angelone, and M. Dalmonte, Gauge-theoretic origin of Rydberg quantum spin liquids, Phys. Rev. Lett. **129**, 195301 (2022).
[57] C. Hickey, C. Berke, P. P. Stavropoulos, H.-Y. Kee, and S. Trebst, Field-driven gapless spin liquid in the spin-1 Kitaev honeycomb model, Phys. Rev. Res. **2**, 023361 (2020).
[58] Z. Zhu, Z.-Y. Weng, and D. N. Sheng, Magnetic field induced spin liquids in $S = 1$ Kitaev honeycomb model, Phys. Rev. Res. **2**, 022047(R) (2020).
[59] X.-Y. Dong and D. N. Sheng, Spin-1 Kitaev-Heisenberg model on a honeycomb lattice, Phys. Rev. B **102**, 121102(R) (2020).
[60] H.-Y. Lee, N. Kawashima, and Y. B. Kim, Tensor network wave function of $S = 1$ Kitaev spin liquids, Phys. Rev. Res. **2**, 033318 (2020).
[61] I. Khait, P. P. Stavropoulos, H.-Y. Kee, and Y. B. Kim, Characterizing spin-one Kitaev quantum spin liquids, Phys. Rev. Res. **3**, 013160 (2021).
[62] K. Fukui, Y. Kato, J. Nasu, and Y. Motome, Ground-state phase diagram of spin-S Kitaev-Heisenberg models, Phys. Rev. B **106**, 174416 (2022).
[63] M. Georgiou, I. Rousochatzakis, D. J. J. Farnell, J. Richter, and R. F. Bishop, Spin-S Kitaev-Heisenberg model on the honeycomb lattice: A high-order treatment via the many-body coupled cluster method, Phys. Rev. Res. **6**, 033168 (2024).
[64] A. Ralko and J. Merino, Chiral bosonic quantum spin liquid in the integer-spin Heisenberg-Kitaev model, Phys. Rev. B **110**, 134402 (2024).
[65] H. Ma, $\mathbb{Z}_2$ spin liquids in the higher spin-S kitaev honeycomb model: An exact deconfined $\mathbb{Z}_2$ gauge structure in a nonintegrable model, Phys. Rev. Lett. **130**, 156701 (2023).
[66] R. Liu, H. T. Lam, H. Ma, and L. Zou, Symmetries and anomalies of Kitaev spin-S models: Identifying symmetry-enforced exotic quantum matter, SciPost Phys. **16**, 100 (2024).
[67] H. Yao and S. A. Kivelson, Exact chiral spin liquid with non-Abelian anyons, Phys. Rev. Lett. **99**, 247203 (2007).
[68] S. Dusuel, K. P. Schmidt, J. Vidal, and R. L. Zaffino, Perturbative study of the Kitaev model with spontaneous time-reversal symmetry breaking, Phys. Rev. B **78**, 125102 (2008).
[69] J. Nasu and Y. Motome, Thermodynamics of chiral spin liquids with Abelian and non-Abelian anyons, Phys. Rev. Lett. **115**, 087203 (2015).
[70] A. Ralko and J. Merino, Novel chiral quantum spin liquids in Kitaev magnets, Phys. Rev. Lett. **124**, 217203 (2020).
[71] C. Hickey, M. Gohlke, C. Berke, and S. Trebst, Generic field-driven phenomena in Kitaev spin liquids: Canted magnetism and proximate spin liquid physics, Phys. Rev. B **103**, 064417 (2021).
[72] P. d'Ornellas and J. Knolle, Kitaev-Heisenberg model on the star lattice: From chiral Majorana fermions to chiral triplons, Phys. Rev. B **109**, 094421 (2024).
[73] L. Savary, Quantum loop states in spin-orbital models on the honeycomb lattice, Nat. Commun. **12**, 3004 (2021).
[74] Y.-X. Yang, M. Cheng, and J.-Y. Chen, Chiral spin liquid in a generalized Kitaev honeycomb model with $\mathbb{Z}_4$ 1-form symmetry, Phys. Rev. B **111**, 035129 (2025).